

Dopant-Atom-based SOI-Transistors by Selective Nanoscale Doping

A. Samanta¹, D. Moraru¹, Y. Kuzuya¹, K. Tyszka^{1,2}, L. T. Anh³,
T. Mizuno¹, R. Jablonski², H. Mizuta^{3,4} and M. Tabe¹

¹Research Institute of Electronics, Shizuoka University, 3-5-1 Johoku, Hamamatsu 432-8011, Japan

²Division of Sensors and Measuring Systems, Warsaw University of Technology, Sw. A. Boboli 8, 02-525 Warsaw, Poland

³School of Materials Science, Japan Advanced Institute of Science and Technology, 1-1 Asahidai, Nomi 923-1292, Japan

⁴Nano Group, ECS, Faculty of Physical and Applied Sciences, University of Southampton, Southampton, United Kingdom

Abstract

We fabricated QDs consisting of multiple-phosphorus-donors in Si nano-channels using a conventional selective doping technique, and observed electron tunneling transport through donor-atom-induced discrete states.

1. Introduction

In recent years, single-electron tunneling via single dopants working as quantum dots (QDs), typically in nanoscale SOI-MOSFETs, has been reported [1-5]. In most of the past works, doping was done using conventional techniques that lead to random dopant positions and appropriate devices showing single-dopant characteristics were picked up from many devices. Although several works addressed the precise control of dopant atoms in number by single-ion implantation [6] and of atomic position by scanning tunneling microscope [7], they are state-of-the-art techniques and still far from practical Si technology.

Here, we report, for the first time, i) the formation of QDs consisting of multiple-phosphorus-donors in Si nano-channels using an optimized conventional selective doping technique, and ii) electron transport through donor-atom-induced discrete states. These results are supported by *ab initio* atomistic simulations and Kelvin probe force microscope (KFM) measurements of the potential profile.

2. Selectively-doped nano-channel SOI-MOSFET

The devices investigated in this work are SOI-MOSFETs with a thin Si layer (~5 nm), as shown in Fig. 1(a). The device constriction channel was selectively doped in slit patterns [Fig. 1(b)] using a technique combining precise electron beam lithography with thermal diffusion doping ($N_D \cong 5 \times 10^{18} \text{ cm}^{-3}$). Gate oxidation after doping was performed by lower-temperature wet oxidation, not by dry oxidation, in order to minimize lateral diffusion of dopants. For these conditions, it is expected that a number of P donors are contained within the doped-slit region, leading to formation of QDs. Reference devices, with the channel doped with multiple slits [as shown in Fig. 1(c)], have also been fabricated for Kelvin probe force microscope (KFM) measurements of the electronic potential profile.

3. Tunneling transport in selectively-doped nano-FETs

The devices were characterized by electrical measurements. In Fig. 2, I_D - V_G characteristics for a reference nominally undoped-channel device (illustrated in inset) are shown. These characteristics show a gradual increase of the current level, without significant peaks.

Figures 3(a) and 3(b) show the I_D - V_G characteristics for slit-doped devices with different channel widths (~10 and

~100 nm, respectively) for several low temperatures. For the device with a narrow channel, Fig. 3(a) shows that, at the lowest temperature ($T = 6 \text{ K}$), there is practically no obvious current peak at low V_G 's. However, at $T = 10 \text{ K}$, a prominent current peak can be observed at $V_G \cong 1.6 \text{ V}$. Within the tail of this peak, several sub-peaks (indicated by arrows) can also be identified. These sub-peaks can be traced even at higher temperature (as indicated by dashed lines), although the features become obscure as temperature is increased. The device with wider channel [Fig. 3(b)] exhibits a similar behavior, but with a significantly larger number of sub-peaks corresponding to a larger number of dopant atoms in the slit region.

The first prominent current peak observed at the lower V_G 's corresponds to single-electron tunneling for the lower electron occupancy of the QD. The sub-peaks are thus ascribed to tunneling modulation due to the presence of a discrete density-of-states (DOS) spectrum in the multiple-donor QD, as schematically presented in the Fig. 4. The second current peak, at higher V_G 's, is most likely due to the tunneling transport with one electron already present in the QD, along the Coulomb blockade theory. For the devices with wider channels, the QDs likely contain a larger number of donors, leading to more complex sub-structure.

4. *Ab initio* simulation: single- and multiple-donor FETs

In order to observe the electronic states of coupled donors in nanoscale Si channels, we performed *ab initio* atomistic simulations for single- and multiple-donors systems, as shown in Fig. 5 (upper panels). Channel dimensions are ~2 nm, smaller than for experimental devices.

The lower panels of Fig. 5 show the projected density of states at the central P donor, for an energy range close to the conduction band edge. A single lowest peak can be identified as the donor's ground state for the single-donor nanostructure. With increasing the number of donors, multiple levels can be observed, suggesting a correlation with the number of donors. These findings provide basic support and insight for experimental results.

5. KFM measurement of selectively-doped FETs

For observing the electronic potential of slit-doped FETs, a KFM technique was used on reference multiple-doped-slits device. Here, we show in Fig. 6 the electronic potential image for an area focused around one slit. It can be seen that, for the doped slit (as indicated in the figure), the electronic potential is lower, consistent with the presence of ionized P donors. This suggests successful formation of local slit-doped channels.

6. Conclusions

We presented the electrical characteristics of selectively-doped nano-channel SOI-transistors, supported by KFM potential measurements. Further insights on the role of single and multiple donors in nanoscale transistors are provided by *ab initio* simulation of the devices.

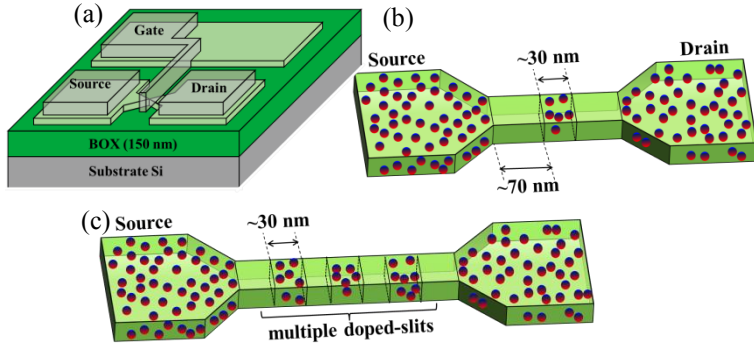


Fig. 1. (a) Bird-eye view of SOI-MOSFETs under study. (b) Illustration of possible dopant distribution of a selectively-doped single-slit SOI-MOSFET. (c) Multiple-slits selectively-doped device for KFM measurement.

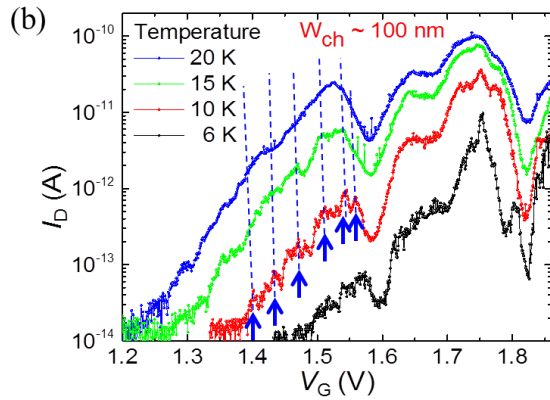
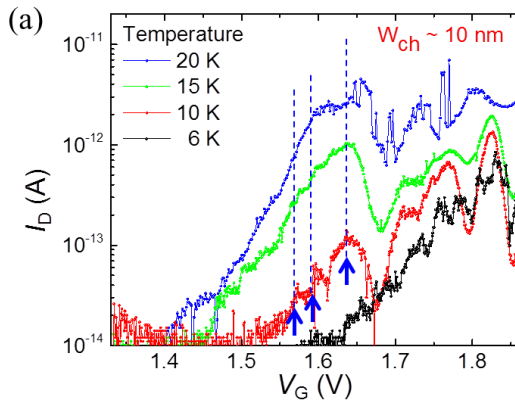


Fig. 3. Temperature dependence of I_D - V_G measurements for selectively-doped-channel SOI-MOSFETs (designed slit width ~ 30 nm and undoped gap ~ 70 nm) with different channel widths: (a) 10 nm and (b) 100 nm. Sub-peaks (inflections) embedded within the envelope of the first peak are indicated by arrows and dashed lines.

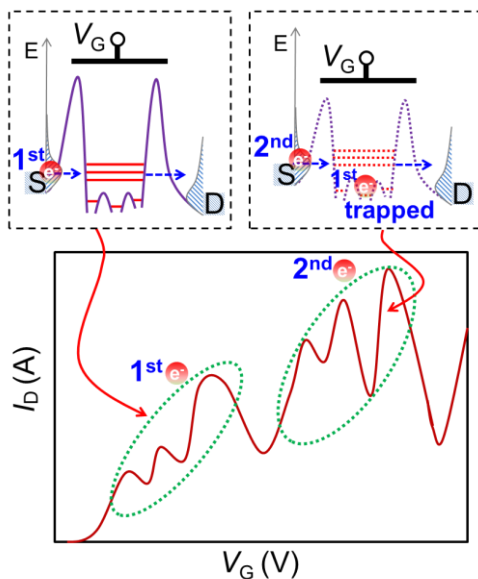


Fig. 4. Single-electron tunneling via excited states of a QD containing clustered multiple phosphorus-dopants in selectively-doped nano-channel SOI-MOSFET. Peaks due to consecutive electron occupancies are illustrated.

References

- [1] H. Sellier *et al.*, Phys. Rev. Lett. **97** (2006) 206805.
- [2] Y. Ono *et al.*, Appl. Phys. Lett. **90** (2007) 102106.
- [3] M. Pierre *et al.*, Nature Nanotechnol. **5** (2010) 133.
- [4] M. Tabe *et al.*, Phys. Rev. Lett. **105** (2010) 016803.
- [5] E. Hamid *et al.*, Phys. Rev. B **87** (2013) 085420.
- [6] E. Prati *et al.*, Nature Nanotechnol. **7** (2012) 443.
- [7] M. Fuechsle *et al.*, Nature Nanotechnol. **7** (2012) 242.

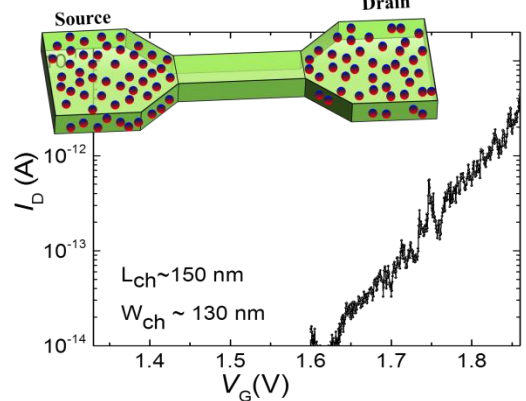


Fig. 2. Representative I_D - V_G characteristics of nominally-undoped device (as shown in inset), measured at $T = 6$ K. No significant current peak can be observed.

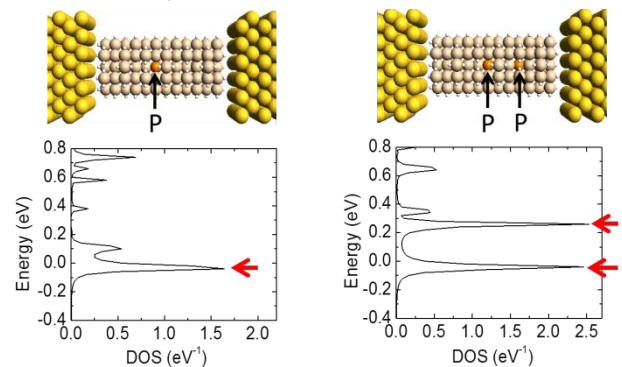


Fig. 5. Atomistic views of device structure (upper panels) and projected density of states (PDOS) spectra at the center P donor (lower panels) for: (a) single- and (b) double-donors systems.

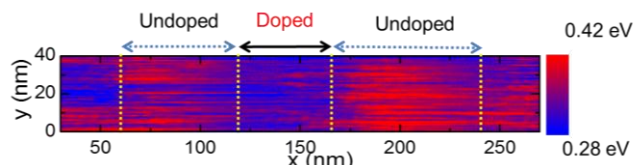


Fig. 6. Electronic potential map of one selectively-doped slit in a multiple-slits channel measured by Kelvin probe force microscope.